A Study of Two-Wheel Vehicle Dynamics with Constant Speed

Der-Cherng Liaw, Chien-Chih Kuo, Yi-Tien Hung and Yi-Ming Hu

Abstract—**This study explores the possible dynamical motions for a two-wheel vehicle with constant speed. Both of sufficient and necessary conditions for the existence of circular motion are obtained. Nine types of possible motion for two-wheel vehicle are then deduced from the obtained necessary condition. Numerical simulations are also given to demonstrate the analytical results and the usage of constant speed control for two-wheel vehicle's motion.**

Index Terms—**Circular motion, vehicle, dynamics.**

I. INTRODUCTION

Due to the rapid development of electronic technology, the research of smart cars has recently attracted lots of attention, especially in self-driving cars. Among those studies, Google Company has developed a self-driving car for road testing. It can also be seen from the literatures that autonomous driving technology can reduce the accident, relax the impact of traffic congestion and improve the safety of vehicle driving [1]. In the study of the dynamical behavior of vehicle dynamics, lots of results have been presented to find possible causes of making traffic accidents and enhance the driving safety for automated steering vehicle (e.g., [2]-[4]).

Several control schemes have been proposed for the guidance and/or motion control of vehicle or mobile robot (e.g., [5]-[10]). Among those studies, Song and Li [8] developed an LQR controller from a linear state space model. In their demonstrations, tracking errors can be eliminated and the mobile robot can follow a specified trajectory. The addition of nonlinear control for mobile robot can be solved by using discontinuous feedback and variable continuous feedback control laws [9]-[10].

Most of existing vehicles on the road are known to have four wheels, which makes the vehicle hard to turn with small radius. In this paper, we will extend the study of two-wheel vehicle presented in [8] for finding its possible dynamical motion with constant speed. The analytical results will reveal that the two-wheel vehicle can exhibit self-spinning motion which is hard for the vehicle with four wheels.

The paper is organized as follows. In Section II, we will first recall a result on the decision of periodic solution for the given dynamical system from [9]. It is followed by the derivation of necessary and sufficient conditions for the existence of circular motion for the two-wheel vehicle dynamics with constant speed. Numerical simulations will be

D.-C. Liaw, Institute of Electrical and Control Engineering, National Chiao Tung University, 1001 Ta Hsueh Road, Hsinchu, Taiwan, R.O.C.
C.-C. Kuo, Institute of Electrical and Control Engineering, National Chiao Tung University, 1001 Ta Hsueh Road, Hsinchu, Taiwan, R.O.C.
Y.-T. Hung, Institute of Electrical and Control Engineering, National Chiao Tung University, 1001 Ta Hsueh Road, Hsinchu, Taiwan, R.O.C.
Y.-M. Hu, Institute of Electrical and Control Engineering, National Chiao Tung University, 1001 Ta Hsueh Road, Hsinchu, Taiwan, R.O.C.

given in Section IV to demonstrate the analytical results and the usage of the obtained necessary conditions. Finally, concluding remarks are given in Section V.

II. PRELIMINARY

In the following, a condition for the occurrence of the orbital motion will be recalled from [11]. The result will then be used in Section III for the study of the condition for possible circular motion exhibited on a two-wheel dynamics.

Consider a two-dimensional system as given in Eqs. (1)-(2) below:

$$\dot{x}_1 = f_1(x_1, x_2), \tag{1}$$

$$\dot{x}_2 = f_2(x_1, x_2), \tag{2}$$

where $(x_1, x_2) \in \Re^2$ and f_1, f_2 are assumed to be two smooth functions of x_1 and x_2. Suppose we can find a continuous and differentiable function $V(x_1, x_2)$ such that

$$\dot{V}(x_1, x_2) \triangleq \frac{\partial V}{\partial x_1} f_1(x_1, x_2) + \frac{\partial V}{\partial x_2} f_2(x_1, x_2) = 0. \tag{3}$$

Denote $\mathbb{C}$ the solution trajectory of system Eqs. (1)-(2) originating at the initial $\left[x_1(0), x_2(0)\right]^T$. By Eq. (3), the time derivative of $\dot{V}\left[x_1(t), x_2(t)\right]$ is zero along $\mathbb{C}$, so that $V\left[x_1(t), x_2(t)\right]$ is constant along $\mathbb{C}$. Let the set S be defined by

$$S = \left\{(x_1, x_2) : V\left[x_1(t), x_2(t)\right] = V\left[x_1(0), x_2(0)\right]\right\} \quad \forall t \geq 0. \tag{4}$$

It is clear that $\mathbb{C}$ is a subset of S. Thus, we can conclude that the system will have a closed trajectory solution when S is a closed curve. Details are given in Proposition 1 below.

Proposition 1: Suppose there exists a continuous and differentiable function V such that the condition given in Eq. (3) holds. Then the system (1)-(2) will exhibit a closed trajectory if $V(x_1, x_2) = c \geq 0$ is a closed curve.

III. ANALYSIS OF TWO-WHEEL VEHICLE DYNAMICS

Consider a two-wheeled vehicle model as depicted in Fig. 1. The corresponding motion equation can be adopted from [8] as given in Eqs. (5)-(7) below:

$$\dot{x} = V_p \cdot \cos\theta, \tag{5}$$

$$\dot{y} = V_p \cdot \sin\theta, \tag{6}$$

$$\dot{\theta} = \omega = \frac{V_R - V_L}{2L}. \tag{7}$$

Here, x, y, and θ are system states, V_P, V_L and V_R denote the speeds of the vehicle, the left wheel and the right wheel, respectively. In addition, θ is the angle between vehicle's heading direction and the X-axis, ω represents the yaw rate of the vehicle, P denotes the center of mass and L is the half width of the vehicle. By the definition, it is clear that we have $V_P = (V_R + V_L) / 2$.
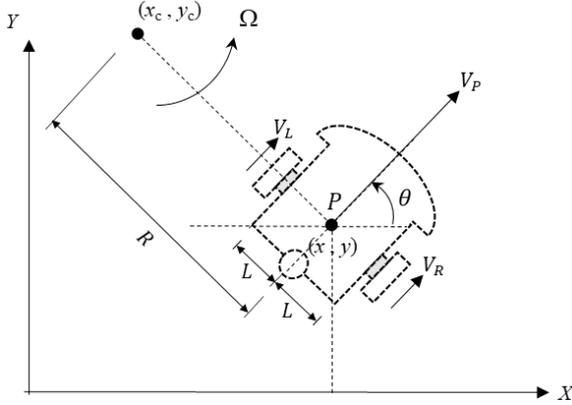

Fig. 1 Two-wheeled vehicle model

In the following, we will study the possible dynamical motion of the vehicle system (5)-(7) with constant speed. That is, the values of V_R and V_L are both constant.

It is clear from Eqs. (5)-(6) that we have the following relationship:

$$\theta = \tan^{-1} \frac{\dot{y}}{\dot{x}}. \tag{8}$$

That means, the motion of θ will also depends on Eqs. (5)-(6). In the following analysis, we will focus on the dynamics given in (5)-(6) only.

First, we consider the necessary condition of circular motion for the vehicle system (5)-(7). Suppose the two-wheel vehicle will exhibit a circular motion. Let (x_c, y_c) denote the center of the assumed circular motion and Ω be the corresponding angular velocity, respectively, as shown in Fig. 1. It is observed from Fig. 1 that we can have the following relationships:

$$V_R = (R + L)\Omega, \tag{9}$$
$$V_L = (R - L)\Omega. \tag{10}$$

The two equations above lead to the next relationship: $V_R(R - L) = V_L(R + L)$. So, we can have $V_R = \mu \cdot (R + L)$ and $V_L = \mu \cdot (R - L)$ for some constant $\mu \in \Re$. Based on the discussions above, then we have the following necessary condition.

Lemma 1. Suppose the vehicle exhibits circular motion. Then we have the following conditions:
(i)   If the circular motion becomes linear motion, i.e., $R = \infty$, then $V_R = V_L$.
(ii) If the circular motion becomes a self-spinning motion, i.e., $R = 0$, then $V_R = -V_L$.
(iii) If the circular motion has finite radius, $0 < R < \infty$, then the values of V_R and V_L can be selected as

$$V_R = \mu \cdot (R + L) \quad \text{and} \quad V_L = \mu \cdot (R - L) \quad \text{for some constant } \mu \neq 0.$$

Note that, the sign and the magnitude of μ in Lemma 1 determine the direction and the angular speed of the circular motion, respectively. In fact, $\mu > 0$ (i.e., $V_R > V_L$) corresponds to counterclockwise motion, while $\mu < 0$ (i.e., $V_R < V_L$) associates with clockwise motion.

Next, we consider the sufficient condition of circular motion for the vehicle system (5)-(6).

Choose $V(x, y)$ as defined in Eq. (11) below:

$$V(x, y) = (x - x_c)^2 + (y - y_c)^2, \tag{11}$$

where (from Fig. 1)

$$x_c = x - R\cos\left(\frac{\pi}{2} - \theta\right), \tag{12}$$

$$y_c = y + R\sin\left(\frac{\pi}{2} - \theta\right). \tag{13}$$

It is clear that the set of (x, y) that satisfies $V(x, y) \equiv R^2$ is a closed curve.

Now, we apply the function V to Eqs. (5)-(6). We then have

$$\begin{aligned}
\dot{V} &= 2\left[(x - x_c) \cdot \dot{x} + (y - y_c) \cdot \dot{y}\right] \\
&= 2\left[R\cos\left(\frac{\pi}{2} - \theta\right) \cdot V_P \cos\theta - R\sin\left(\frac{\pi}{2} - \theta\right) \cdot (V_P \sin\theta)\right] \\
&= 2\left[R\sin\theta(V_P \cos\theta) - R\cos\theta(V_P \sin\theta)\right] \\
&= 0. \tag{14}
\end{aligned}$$

The next result follows readily from Proposition 1.

Lemma 2. The vehicle system (5)-(7) will exhibit circular motion if the values of V_R and V_L are both constant.

Note that, the relation between ω and Ω can also be calculated as given below:

$$\omega = \frac{V_R - V_L}{2L} = \frac{(R + L)\Omega - (R - L)\Omega}{2L} = \Omega. \tag{15}$$

IV. SIMULATION RESULTS

In this section, we will construct numerical results by using code Matlab to demonstrate the analytical results obtained in Section II. First, we will consider all possible typical vehicle motions described in Lemma 1. Two examples of specified motion will then be constructed by using those typical motions to demonstrate the usage of constant speed control for two-wheel vehicle's motion.

A. Typical vehicle motion

First, we present the numerical results for the motion of the center of mass P. In the following simulations, we assume

that $L = 1.8\,(m)$ and $V_R = 5\,(m/s)$. The simulation results for the motion of the center of mass P with different values of V_L are shown in Fig. 2. It is observed from Fig. 2 that the trajectory is a clockwise circle if $V_R < V_L$ or a counterclockwise circle if $V_R > V_L$. In addition, the trajectory will be a straight line if $V_R = V_L$. The numerical results shown in Fig. 2 agree with those given in Lemmas 1 and 2. Moreover, from Eq. (15), the bigger the value $|V_R - V_L|$ is, the larger the angular speed $|\omega|$ or $|\Omega|$ is.
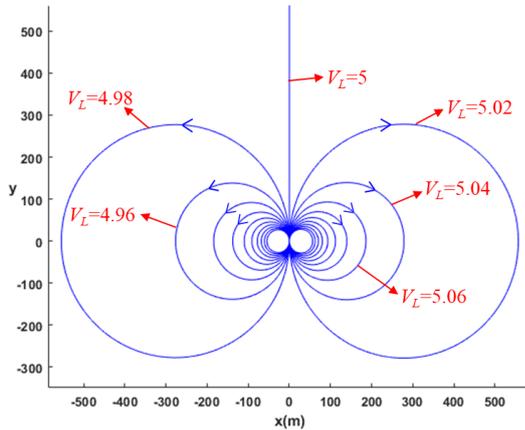
Fig. 2 motion of the center of mass P with $V_R = 5(m/s)$ and various value of $V_L(m/s)$.

Next, we consider the motions of two wheels and the center of mass P with respect to different setting values of wheel speed.

Consider an inertial coordinate system with the initial position of the point P being at the origin (0,0). The initial heading of the vehicle is set to be $\pi/2$. Here, we consider three different values of V_L with $V_L = 0\,(m/s)$, $V_L = 2\,(m/s)$ and $V_L = -2\,(m/s)$, respectively. Details are given below.

Case 1. $V_L = 0\,(m/s)$

In the simulation result of $V_L = 0\,(m/s)$, the motion of the point P is stationary point when the right wheel speed is 0. However, the motion of the point P is either counterclockwise spin or clockwise spin when the right wheel speed is positive or negative, respectively. Details are depicted in Fig. 3.
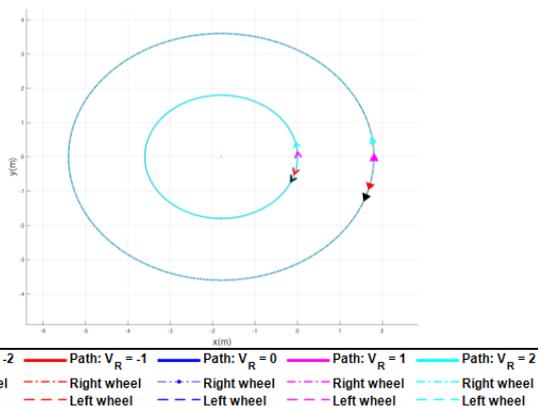

Fig. 3 Simulation results of the left and right wheel trajectories for $V_L = 0(m/s)$ and various value of $V_R(m/s)$

Case 2. $V_L = 2\,(m/s)$

In the simulation result of $V_L = 2\,(m/s)$, the vehicle motion is forward linear motion when the right wheel speed is also $2(m/s)$. However, when $V_R > V_L$ or $V_R < V_L$, the vehicle produces a clockwise or counterclockwise rotary motion with a radius, respectively. When $V_R < 0$, as shown in Fig. 4 the rotational motion radius will be less than L of which $V_R = 0\,(m/s)$. Moreover, the vehicle will produce clockwise spin motion when $V_R = -V_L$. The timing responses of the left-wheel P_L, right-wheel P_R and the center of mass P in X-Y coordinate for $V_R \leq 0$ are given in Fig. 5, respectively.
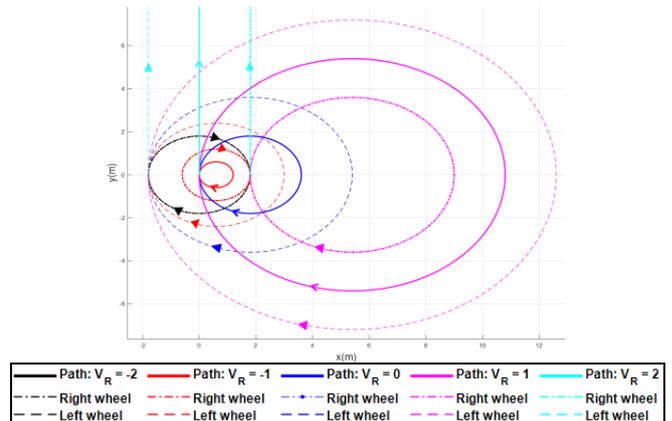

Fig. 4 Simulation results of the left and right wheel trajectories at $V_L = 2(m/s)$ and various value of $V_R(m/s)$
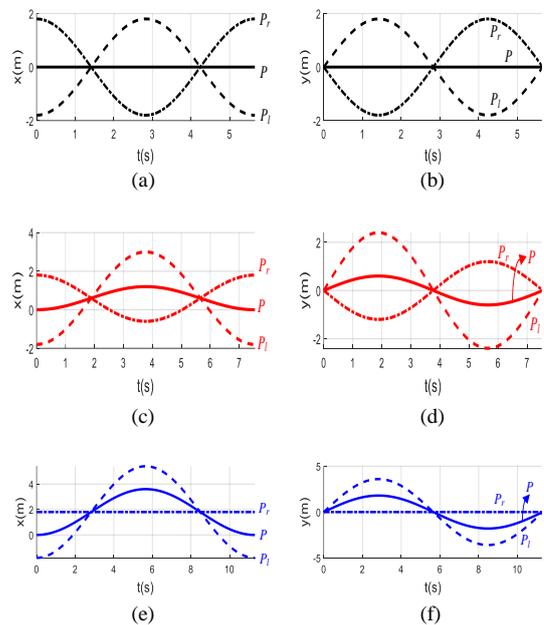

Fig. 5 Vehicle trajectories at $V_L = 2(m/s)$.
X-t plot at (a) $V_R = -2(m/s)$; (c) $V_R = -1(m/s)$; (e) $V_R = 0(m/s)$.
Y-t plot at (b) $V_R = -2(m/s)$; (d) $V_R = -1(m/s)$; (f) $V_R = 0(m/s)$.

Case 3. $V_L = -2\,(m/s)$

Simulation results for $V_L = -2\,(m/s)$ are obtained as depicted in Fig. 6 and 7. It can be found that those trajectories are opposite to the ones shown in Fig. 4 and 5 for $V_L = 2\,(m/s)$.
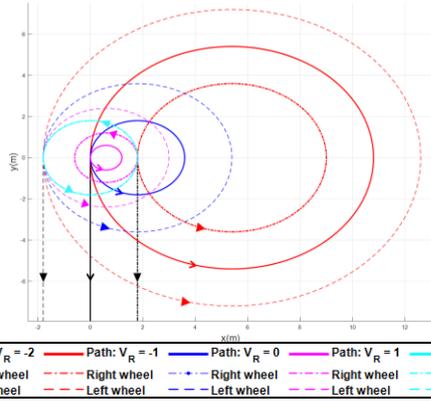
Fig. 6 Simulation results of the left and right wheel trajectories at $V_L = -2(m/s)$ and various value of $V_R(m/s)$
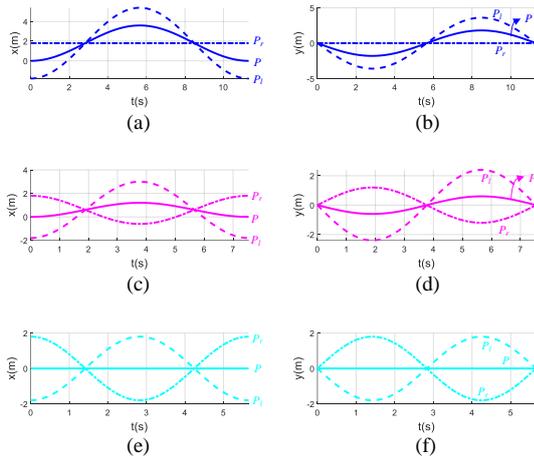

Fig. 7 Vehicle trajectories at $V_L = -2(m/s)$.
X-t plot at (a) $V_R = 0(m/s)$; (c) $V_R = 1(m/s)$; (e) $V_R = 2(m/s)$.
Y-t plot at (b) $V_R = 0(m/s)$; (d) $V_R = 1(m/s)$; (f) $V_R = 2(m/s)$.

Based on the simulation results presented above, we can summarize the possible typical motion of two-wheel vehicle as listed below:

(i) When $|V_R| < -V_L$, the vehicle performs a counterclockwise circular motion on the right half plane of the coordinate y-axis. Two examples are shown in Fig. 8.

(ii) When $|V_R| < V_L$, the vehicle performs a clockwise circular motion on the right half plane of the coordinate y-axis. Two examples are shown in Fig. 9.

(iii) When $V_R > |V_L|$, the vehicle performs a counterclockwise circular motion on the left half plane of the coordinate y-axis. An example is shown in Fig. 10(a).

(iv) When $-V_R > |V_L|$, the vehicle moves clockwise in the left half plane of the coordinate y-axis. An example is shown in Fig. 10(b).

(v) When $V_R = -V_L$, $V_R > 0$ and $V_L < 0$, the vehicle spins counterclockwise at the origin of the coordinates. An example is in Fig. 11(a).

(vi) When $V_R = -V_L$, $V_R < 0$ and $V_L > 0$, the vehicle spins clockwise at the origin of the coordinates. An example is shown in Fig. 11(b).

(vii) When $V_R = V_L$, $V_R > 0$ and $V_L > 0$, the vehicle moves linearly in the positive direction of the y-axis on the

coordinates. An example is shown in Fig. 12(a).

(viii) When $V_R = V_L$, $V_R < 0$ and $V_L < 0$, the vehicle moves linearly in the negative direction of the y-axis on the coordinates. An example is shown in Fig. 12(b).
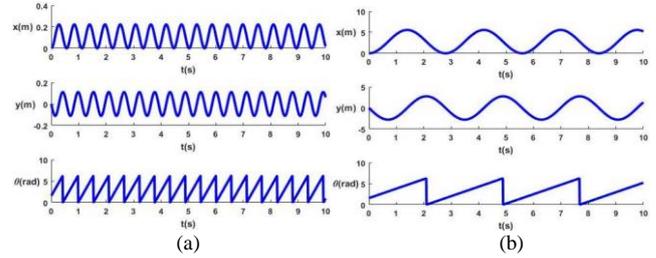

Fig. 8 Vehicle time response diagram at V_L = -7.5(m/s).
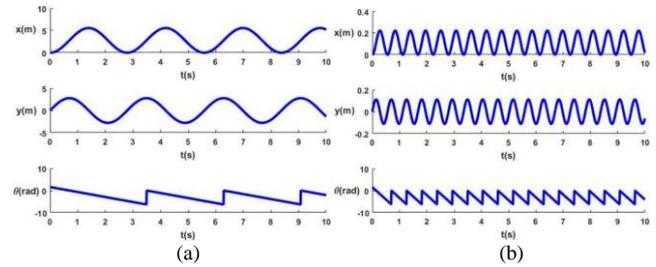(a) $V_R = 5(m/s)$; (b) $V_R = -5(m/s)$

Fig. 9 Vehicle time response diagram at $V_L = 7.5(m/s)$.
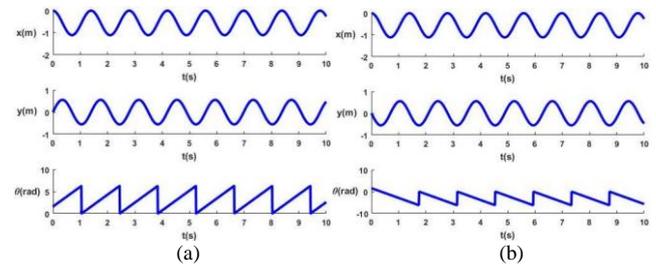(a) $V_R = 5(m/s)$; (b) $V_R = -5(m/s)$

Fig. 10 Vehicle time response diagram at $V_L = 0(m/s)$.
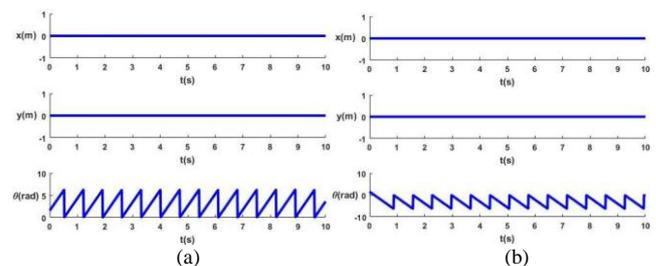(a) $V_R = 5(m/s)$; (b) $V_R = -5(m/s)$

Fig. 11 Vehicle time response diagram
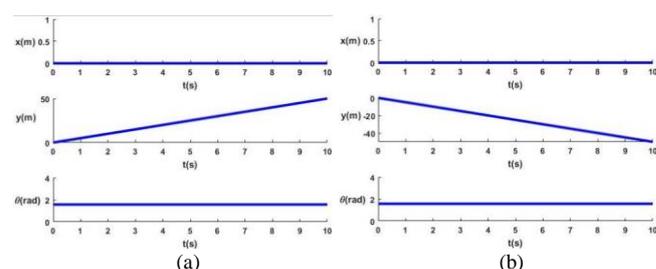(a) $V_L = -5(m/s), V_R = 5(m/s)$; (b) $V_L = 5(m/s), V_R = -5(m/s)$

Fig. 12 Vehicle time response diagram
(a) $V_L = 5(m/s), V_R = 5(m/s)$; (b) $V_L = -5(m/s), V_R = -5(m/s)$

According to the discussions above, we can characterize nine types of possible motion for two-wheel vehicle with constant speed as defined in Fig. 13 and Table 1. This includes the type V for "halt" motion when both values of V_R and V_L are zero. The relationship of the motion type with respect to the values of V_R and V_L is shown in Fig. 14.
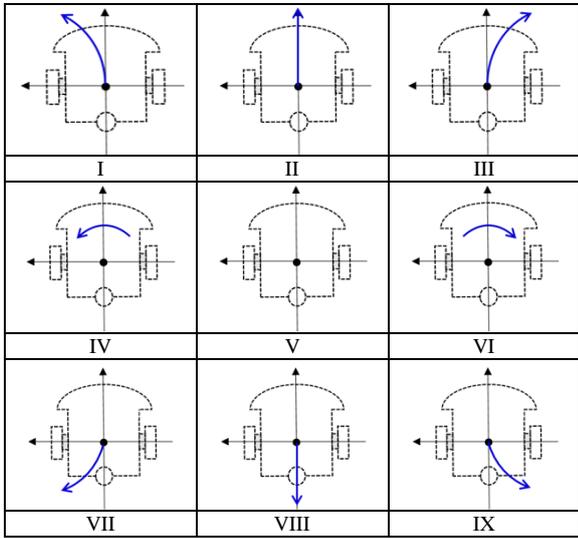

Fig. 13 Motion type

Table 1 Motion type description

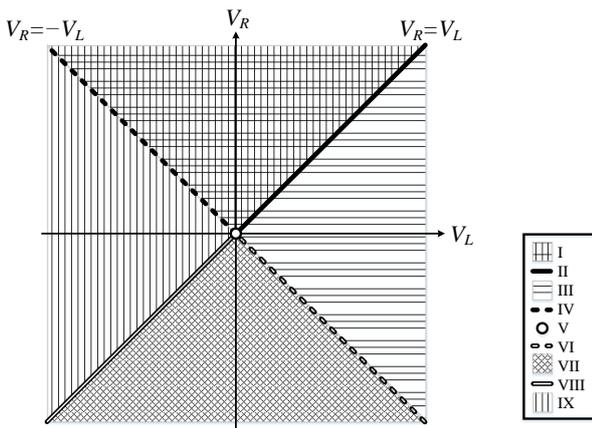| Type	Description
Type I	Turn left forward
Type II	Straight forward
Type III	Turn right forward
Type IV	counterclockwise self-spin
Type V	halt
Type VI	clockwise self-spin
Type VII	Turn left backward
Type VIII	Straight backward
Type IX	Turn right backward

Fig. 14 motion type with respect to V_R and V_L

B. Specified motion

In this section, two examples of specified motion will be constructed by using those typical motions presented above to demonstrate the usage of constant speed control for two-wheel vehicle's motion.

The first example is a path consisting of two semicircles

and straight lines as depicted in Fig. 15. Such a motion is not difficult to achieve. The corresponding simulation procedure is discussed below.
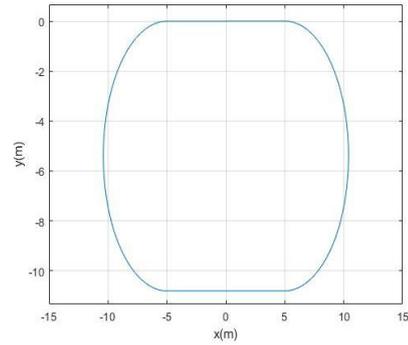

Fig. 15 Specify path 2

Assume the initial position of the vehicle is at the origin (0,0) and the initial heading of the vehicle is 0. The simulation procedure can then be constructed as follows:

(i) $V_L = 1, V_R = 1$: Type II, forwards to (5, 0).

(ii) $V_L = 2, V_R = 1$: Type III, turns right π radians with radius $R = 5.4$.

(iii) $V_L = 1, V_R = 1$: Type II, forwards to (-5, -10.8).

(iv) $V_L = 2, V_R = 1$: Type III, turns right π radians with radius $R = 5.4$.

(v) $V_L = 1, V_R = 1$: Type II, forwards to (-5, 0).

(vi) $V_L = 0, V_R = 0$: Type V, halts at (-5, 0).

The simulation results are shown in, which can be divided into five segments and represented by different colors. The trajectory of the center of mass P is denoted as solid line while the right wheel trajectory is a dash-dot line and the left wheel trajectory is a dashed line, respectively. It is found from Fig. 16 that the trajectory of the center of mass P agrees with the specified path given in Fig. 15.
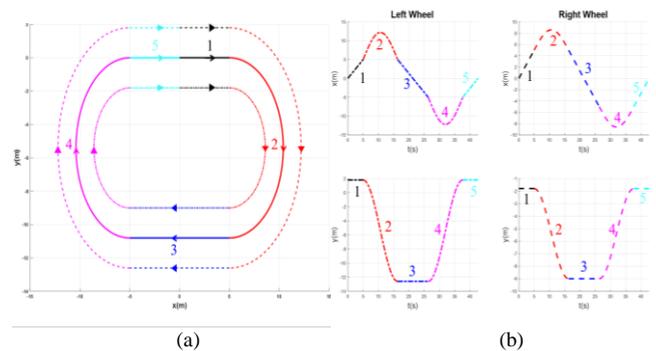

Fig. 16 Trajectory simulation result.
(a) Trajectory simulation (b) Time response of trajectory

The second example of motion is depicted in Fig. 17, which is an 8-alike shaped path with sharp turning angle on the four corners. In general, it is hard for a three-wheel or four-wheel vehicle to exhibit such a motion. However, due to the fact of owning self-spinning type of motion self-spin as discussed above, it is not difficult for two-wheel vehicle to fulfill the task. Details are given below.
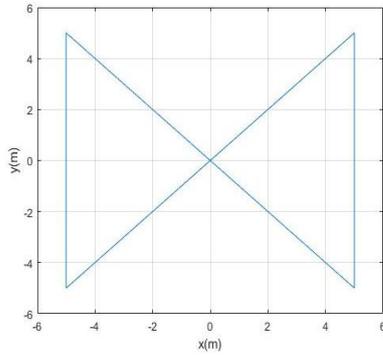
Fig. 17 Example path 1

Assume the initial position of the vehicle is at the origin (0,0) and initial heading of the vehicle is $\pi / 4$. We can now construct the motion by using nine types of motion defined in Fig. 13 to fulfill the requirements. The simulation procedure is as follows:

(i) $V_L = 1, V_R = 1$: Type II, forwards to (5, 5).

(ii) $V_L = 1, V_R = -1$: Type VI, clockwise self-spins $3\pi/4$ radians.

(iii) $V_L = 1, V_R = 1$: Type II, forwards to (5, -5).

(iv) $V_L = 1, V_R = -1$: Type VI, clockwise self-spins $3\pi/4$ radians.

(v) $V_L = 1, V_R = 1$: Type II, forwards to (-5, 5).

(vi) $V_L = -1, V_R = 1$: Type IV, counterclockwise self-spins $3\pi/4$ radians.

(vii) $V_L = 1, V_R = 1$: Type II, forwards to (-5, -5).

(viii) $V_L = -1, V_R = 1$: Type IV, counterclockwise self-spins $3\pi/4$ radians.

(ix) $V_L = 1, V_R = 1$: Type II, forwards to the origin (0, 0).

(x) $V_L = 0, V_R = 0$: Type V, halts at the origin (0, 0).

The simulation results are shown in Fig. 18, which can be divided into nine segments except step (x) and represented by different colors. The notations for the trajectories defined in Fig. 16 will be also applied to those in Fig. 18. It is observed from Fig. 18 that the trajectory of the center of mass P is consistent with the specified path defined in Fig. 17.
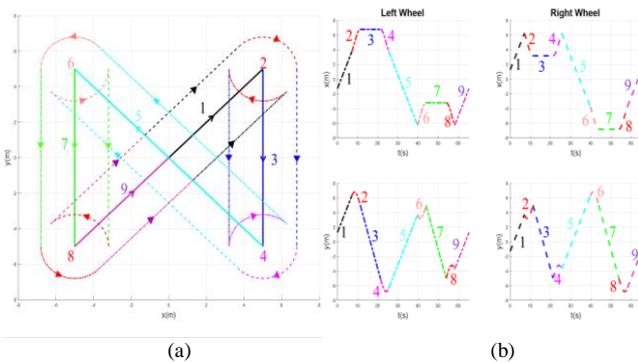

(a) (b)

Fig. 18 Trajectory simulation result
(a) Trajectory simulation (b) Time response of trajectory

V. CONCLUSIONS

In this paper, we have studied the possible dynamical motions for a two-wheel vehicle with constant speed. The necessary and sufficient conditions are also obtained for the existence of circular motion. In addition, numerical simulation results have demonstrated the obtained analytical results and the usage of constant speed control for two-wheel vehicle's motion planning. Those studies can be directly employed to the practical applications.

REFERENCES

[1] T. Vaa, M. Penttinen and I. Spyropoulou, "Intelligent transport systems and effects on road traffic accidents: state of the art," *IET Intelligent Transport Systems*, vol. 1, no. 2, 2007, pp. 81-88.

[2] J. Ackerman, J. Guldner, W. Sienel, R. Steinhauser, and V.I. Utkin, "Linear and nonlinear controller design for robust automatic steering," *IEEE Trans. Control Systems Technology*, vol. 3, no. 1, 1995, pp. 132-143.

[3] L.R. Ray, "Nonlinear state and tire force estimation for advanced vehicle control," *IEEE Trans. Control Systems Technology*, vol. 3, no. 1, 1995, pp. 117-124.

[4] E. Ono, S. Hosoe, H.D. Tuan and S. Doi, "Bifurcation in vehicle dynamics and robust front wheel steering control," *IEEE Trans. Control Systems Technology*, vol. 6, no. 3, 1998, pp. 412-420.

[5] D.-C. Liaw, C.-C. Yua, J.-E. Jhong and C. Tsao, "A design of vehicle's positioning system," *Proc. 2015 The Annual Conference on Engineering and Technology* (*ACEAT 2015*), Nagoya, Japan, Nov. 4-6, 2015.

[6] D.-C. Liaw, C.-H. Tsai, C. Tsao and C.-W. Tung, "A guidance control design for golf-cart," *2016 16th International Conference on Control, Automation and Systems* (*ICCAS 2016*), Gyeongju, Korea, Oct. 16-19, 2016.

[7] D.-C. Liaw, W.-C. Chung and C. Tsao, "Linear control of vehicle's lateral dynamics," *2016 Annual Conference on Engineering and Information Technology* (*ACEAIT 2016*), Kyoto, Japan, 2016.

[8] K. T. Song and C.E. Li, "Tracking control of a fee ranging automatic guided vehicle," *Contr. Eng. Practice*, vol. 1, no. 1, 1993, pp. 163-169.

[9] J. Huang, "Adaptive tracking control design for high-order nonholonomic mobile robot systems," *2008 International Conference on Machine Learning and Cybernetics*, Kunming, 2008, pp. 1866-1871.

[10] G. Zidani, S. Drid, L. Chrifi-Alaoui, A. Benmakhlouf and S. Chaouch, "Backstepping controller for a wheeled mobile robot," *2015 4th International Conference on Systems and Control* (*ICSC*), Sousse, 2015, pp. 443-448.

[11] M. Vidyasagar, *Nonlinear Systems Analysis*, Prentice-Hall, ch. 2, sec. 2.4.5, 1978, pp. 39.

Der-Cherng Liaw, Institute of Electrical and Control Engineering, National Chiao Tung University, 1001 Ta Hsueh Road, Hsinchu, Taiwan, R.O.C.

C.-C. Kuo, Institute of Electrical and Control Engineering, National Chiao Tung University, 1001 Ta Hsueh Road, Hsinchu, Taiwan, R.O.C.

Y.-T. Hung, Institute of Electrical and Control Engineering, National Chiao Tung University, 1001 Ta Hsueh Road, Hsinchu, Taiwan, R.O.C.

Y.-M. Hu, Institute of Electrical and Control Engineering, National Chiao Tung University, 1001 Ta Hsueh Road, Hsinchu, Taiwan, R.O.C.